Asociación Argentina
de Mecánica Computacional

Mecánica Computacional Vol XXXVIII, págs. 1059-1070 (artículo completo)
H.G. Castro, J.L. Mroginski, R.R. Paz, M.A. Storti (Eds.)
Resistencia, 1-5 Noviembre 2021

SPHERICAL STEEL CONTAINMENTS: COLLAPSE MODELLING FOLLOWING THE 1987 GERMAN RESEARCH PROGRAM

José A. Santelli [a], **Nicolás E. Catalá** [b], **Fernando G. Flores** [c]

[a] *Grupo de investigación GITEVE. Centro de Investigación CIDIV, Facultad Regional Gral. Pacheco, Universidad Tecnológica Nacional - Argentina; jsantelli@docentes.frgp.utn.edu.ar, https://www.frgp.utn.edu.ar/*

[b] *Unidad de Gestión Proyectos Nucleares, Nucleoeléctrica Argentina S.A., Villa Martelli, Pcia. de Buenos Aires, Argentina.; ncatala@na-sa.com.ar, http://www.na-sa.com.ar/*

[c] *Instituto de Estudios Avanzados en Ingeniería y Tecnología (IDIT) UNC-CONICET, y Departamento de Estructuras, FCEFYN, Universidad Nacional de Córdoba, Av. Velez Sarsfield 1611 , 5016 Cordoba,Argentina.*; fernando.flores@unc.edu.ar, https://fcefyn.unc.edu.ar/

Keywords: spherical steel containments, plastic collapse, solid finite elements, solid-shell finite elements.

Abstract. In this work, the 1987 physical tests program to research for plastic collapse estimation of the wall on nuclear spherical steel containments, were correlated using several up-to-date finite element formulations (3D and solid-shell). This way, the collapse loads due to plastic instability of spherical steel containments were obtained by FEM modelling. Also, the analytical collapse load for the spherical containment, as stated in ASME BPVC Section III Division I Appendix II, was studied. The findings were that the correlation between the physical tests and the FEM models strongly depends on the hardening law selected for the constitutive model. It was also found that, with the material model parameters properly adjusted, the plastic collapse of the containment can be modelled with acceptable precision, trough the measurement of thickness reduction. Finally, it was found that the collapse loads specified in ASME are more conservative than the ones found in this work.

1 INTRODUCTION

The German PHWR designs (Göller et al., 1987) are constructed inside a spherical steel containment built on 15MnNi63 steel, of approximately 56 m diameter, and 38 mm. wall thickness. The containment is supported by a concrete base, approx. 40º below the equator.

These type of PHWR containments (also built in Argentina), can be described as large free-standing spheres, a particular type of thin-walled structure. This structure, once constructed, has a number of thickness variations trough member panels, several hatch penetrations, and also a large number of piping penetrations. On the containment construction (in compliance with the ASME Boiler and Pressure Vessel Code), these complexities are considered and designed in acceptance of the code. The cited work is, however, focused on the plastic collapse of the wall, which is an accident condition far beyond containment's design loads.

During the design phase, a reference accident pressure of 5 bar is considered for ASME certification. Then, during leakage tests after construction, the pressure increases up to 6.7 bar without any problems in the containment.

A Research Program (Krieg et al., n.d.) was conducted in order to perform a series of physical tests, in order to determine the containment's plastic collapse load in the shell, whether a moderate leakage occurs preventing a future pressure increase, or whether a global failure must be expected causing considerable mechanical damage. The experimental set-up for the tests were plane circular membranes loaded by unilateral pressure up to failure. These scaled test consisted of a membrane of 860 mm diameter with a wall thickness of 2 mm. This physical test reached the pressure of 42.8 bar before failure.

Also, a local work in Argentina, on failure load determination (Sanchez Sarmiento et al., 1985), exists on this matter, on a sphere of 56 m diameter and 30 mm wall thickness, following the 2010 ASME BPVC Section III Division I Appendix II standard, that allows to have an analytical estimation of the collapse load. This ASME estimation allows to establish the point at which the analytical failure occurs, and this way, study the stress state at this condition.

During this work, a further FEM analysis of the scaled test was carried out using 3D-solid current-technology finite elements, and the results are analyzed and reported.

2 DESCRIPTION OF THE 1987 EXPERIMENTAL SET-UP

The setup of the physical experiment is as it shown in the next figure, extracted from (Göller et al., 1987):

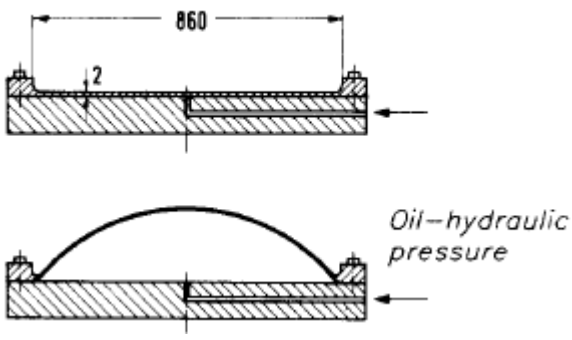

Figure 1. Experimental setup of the membrane test.

The membrane is originally flat, deforming into a shape of spherical section, by means of

hydraulic oil pressure, and bolted all around the external circumference. After a noticeable large strain, the shape of the membrane is approximately a spherical section, and then the failure occurs approximately at the top of the dome.

The experiment result is the plastic collapse (due to a static load) of a spherical membrane of approximately 1 m diameter, with a wall thickness of 1.5 mm.

The ratio R/t (radius by thickness), can be considered as a scale factor, in order to find the containment collapse pressure, based on the results of this physical model.

3 SPHERICAL STEEL CONTAINMENTS AND THE ASME CODE

The ASME Boiler and Pressure Vessel Code sets the rules to which this type of structures must be constructed in compliance. The term 'construction' here includes material, design, fabrication, testing, inspection, etc. (Berman, 1978).

Generally, in the Design Specification, the manufacturer is requested to comply with this Code or any similar in the corresponding country. In essence, these Code rules are mainly based on elastic behavior, short term inelastic behavior, and cyclic behavior.

The criteria of the Code are, above all, the cumulated construction experience: they consist of the best practices in design, analysis, manufacturing, materials, etc.

Mainly, the primary evaluation of safety is made with the stress intensities limited to the elastic range. The primary stress limits are set so as to prevent plastic deformation and to have some safety factor relative to a generally conservative estimate of the ductile burst stress (or perhaps more basically, the yield stress).

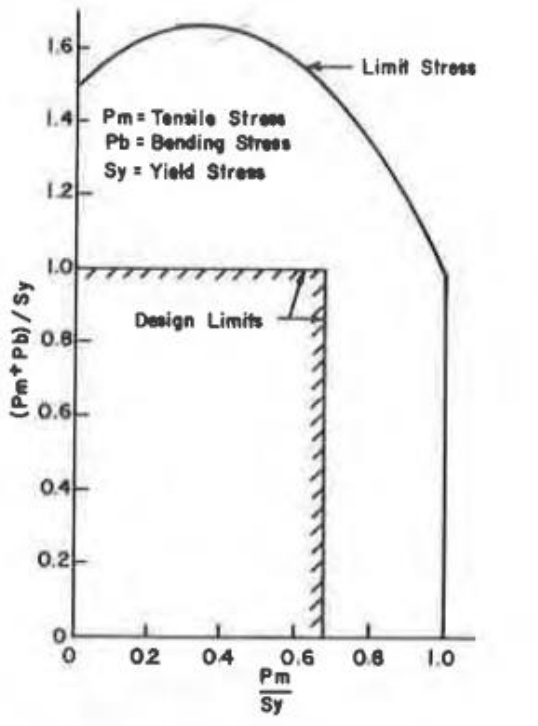

Figure 2. Limit Stress for Combined Tension and Bending

In Figure 2, taken from (The ASME, 1969), the Design Limits are those within the acceptance of the Code. The limit stress, although, are the ultimate load on a uniaxial stress test, this is, the initiation of the necking in a specimen.

Secondly, the Code evaluates the short term inelastic behavior. This is, a small amount of plasticity is allowed, and the vessel 'work hardens' (undergoes work hardening in a few small locations).

In third place, the Code evaluates the cyclic behavior, this means, prevention of phenomena such as ratcheting, etc.

In this work, as well as the referenced physical tests in 1987, the stress levels are found far beyond these limits, because of the nature of a membrane state. In such case, the necking or instability of a membrane occurs at a higher stress level, as we will see in the results.

However, there is a reference of collapse tests in the ASME Code (Sanchez Sarmiento et al., 1985) in ASME Section III, Division I, Mandatory Appendix II, 'Experimental Stress Analysis', 'Criterion for Collapse Load'. In this criterion there is a collapse load point and a collapse Limit Line, which in the case of a membrane state, could be analyzed and compared to the results presented in this work.

4 MODELLING THE PHYSICAL TEST SET-UP WITH SEVERAL FEM CODES

The 1987 plastic collapse test will then be modelled with an up-to-date finite element formulation, following the goal of plastic collapse correlation between the physical tests and the FEM models.

In the case of FEM models, this plastic collapse can be captured by several approaches:

In 1987:

- ROTMEM Code: Calculation of the membrane stresses and strains of an axisymmetric shell under axisymmetric pressure loading. Elastoplastic behavior considered. Large deformations including changes of wall thickness are taken into account. However, bending and shear stresses are neglected. For the numerical treatment, the membrane is described by the coordinates of discrete points of a meridian. The radii of curvature, the tangent angle and the strains of the membrane can easily be determined from these data. Using the deviatoric strains, the deviatoric stresses can be computed by inverting the Prandtl-Reuss equation (Göller et al., 1987).

In this work:

- Implicit 3D finite elements model with material non-linearity using Von Mises failure criteria with Saturation (Voce) hardening law. Large deformations are taken into account.
- Pseudo-static (Explicit) 3D solid-shell finite elements model using Von Mises failure criteria with Saturation (Voce) hardening law. Large deformations are taken into account.

4.1 Main characteristics of the codes used to model the test

In this work, models with current-technology elements were generated, thus allowing a correlation between physical tests and 3D representation of the problem, visualizing the zone with plastic collapse instability in a contour plot form, rather than simply a 2-axis diagram.

This enables a further study of the collapse zone observed in the referenced work and the area shown in the modelisation.

5 IMPLICIT FINITE ELEMENT MODELLING

5.1 SOLID186: 3D solid element type (Ansys)

In this section, the current-technology solid element type formulation in ANSYS code is described:

SOLID186 is a higher order 3-D 20-node (14 integration points) solid element that exhibits quadratic displacement behavior. The element is defined by 20 nodes having three degrees of freedom per node. The element has the capacity to model plasticity, hyperelasticity, creep, stress stiffening, large deflection, and large strains. It also has mixed-formulation capability for simulating deformations of nearly incompressible elastoplastic materials, and fully incompressible hyperelastic materials.

SOLID186 Homogeneous Structural Solid is well suited to modeling irregular meshes (such as those produced by various CAD/CAM systems).

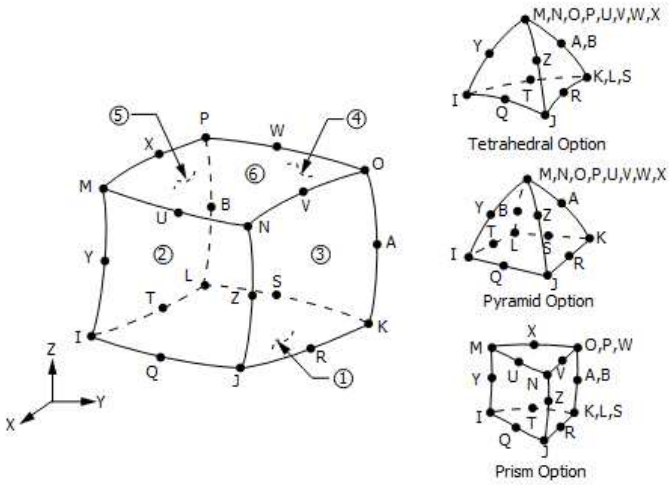

Figure 3 20-node solid element

5.2 Failure criterion, Flow rule, Hardening rule

In this work, the modelling with 3D solid elements will be performed using the following: classical pure displacement formulation, Mises yield criterion, Hencky finite strain tensor, and elasto-plastic constitutive model with Voce isotropic hardening with saturation. As stated previously, the plastic collapse is expected to be captured by the constitutive model only.

In the case of 3D solid-shell finite elements, this remains essentially the same, but with the difference of explicit quasi-static time integration scheme.

5.3 Finite element mesh

In the Figure 4 we can see the 3D hexahedral and wedge mesh:

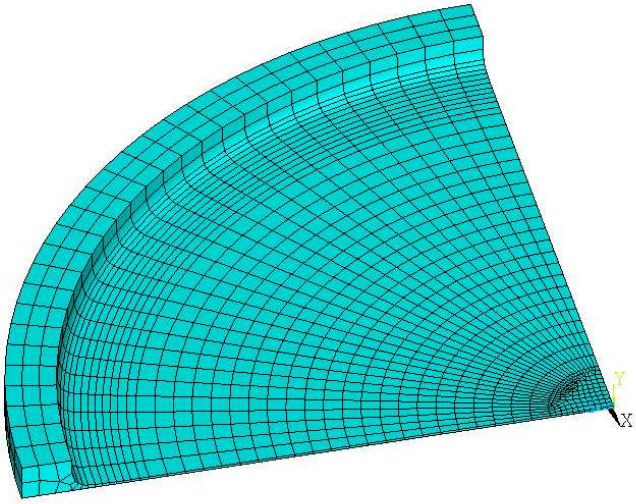

Figure 4. Finite elements mesh of the experimental set-up at initial state. Only a quarter of the model was considered for simulation.

The CAD partitions were made in such a way that the mesh was obtained mostly with hexahedral elements. The model has a total of 2368 hex elements (including 1 wedge), and 9156 nodes. The degenerated element keeps the formulation of SOLID186.

5.4 Boundary conditions

The model is fixed at the bottom thick external ring, and loaded with a pressure of 41,7 Bar in the same side (bottom).

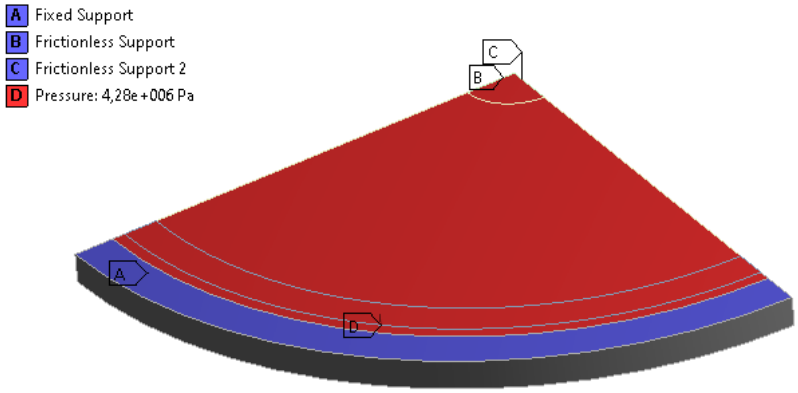

Figure 5. Boundary conditions applied to the model. The view is rotated so the bottom is up.

In Figure 5 we can see all the boundary conditions applied. Fixed support is only applied to the external line of the ring, whereas the blue strip is simply supported. On the red area, we can see the pressure load.

5.5 Solution

The solution method chosen for this case was an implicit Solver, with the NLGEOM (non-linear geometry) option activated (Hencky or logarithmic strain tensor). The strains are computed as the sum of elastic and plastic parts:

$$\{\varepsilon^{tot}\} = \{\varepsilon^{el}\} + \{\varepsilon^{pl}\} \tag{3}$$

The hardening rule can be expressed in the following form:

$$F(\{\sigma\}, k, \{\alpha\}) = 0 \tag{4}$$

Where:
α= back stress (kinematic hardening, not applicable in this case)
k= plastic work

The Solver uses a Backward Euler scheme to enforce that the stress is kept within the yield Surface (by derivative of F in equation (4)):
- Make a first elastic predictor with a trial stress
- If outside the yield surface, start iterating
- Part of that trial strain will become plastic trough the iterative process (plastic strain increment). The Solver calculates this increment in the plastic multiplier λ by means of a local Newton-Raphson procedure (that solves the consistency equation).
- Determines the plastic strain increment:

$$\{d\varepsilon_{pl}\} = \lambda\{\frac{dQ}{d\sigma}\} \tag{5}$$

- Updates the data and moves to the next time increment (which is calculated and varies automatically).

5.6 Material definition

In this section, the constitutive model and the hardening rule will be defined.

The elastic behavior of the material is linear isotropic, with the corresponding values of E and υ. The plastic behavior is modeled with Mises failure criteria and associative flow rule, and the hardening rule is described in more detail in the next section.

Hardening rule:15MnNi63 steel: Voce Law Nonlinear Isotropic Hardening

The Voce hardening model consists of the sum of three terms: a threshold value, a linear term that keeps its rate once saturated, and the saturation term that starts with a strong slope and then saturates, remaining the linear term only.

The evolution of the yield stress for this model is specified by the following equation:

$$\sigma_y = \sigma_0 + R_0\varepsilon^{pl} + R_\infty(1 - \exp(-b\varepsilon^{pl})) \tag{2}$$

where **R**∞ is the difference between the saturation stress and the initial yield stress, **R0**, the slope of the saturation stress and, **b**, the hardening parameter that governs the rate of saturation of the exponential term.

This non-linear isotropic hardening model was tested among the Power Law model, both formulated in a way that the code allows to enter the parameters and without the need of a curve.

The exponential saturation term in this Voce model is expected to capture the phenomenon of membrane thickness 'necking'.

Based on the yield and ultimate stress of the 15MnNi63 steel, the following curves were obtained:

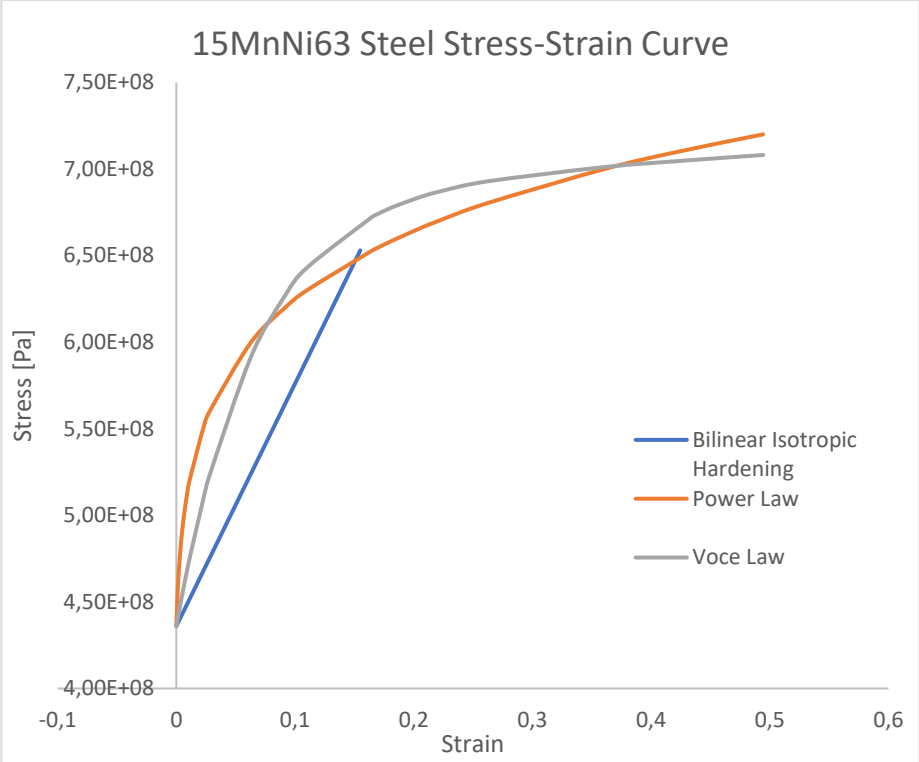

Figure 6. Stress-Strain curves for 15MnNi63 steel at high strains (up to 60%). These curves were obtained by equations (tensile test usually reach around 20% of strain).

In the previous figure, we can see that the Voce law tends to saturation after approx. 30% of plastic strain, which will represent the shell thickness 'necking' more accurately.

5.7 Results (Implicit solution)

Now the model results are presented:

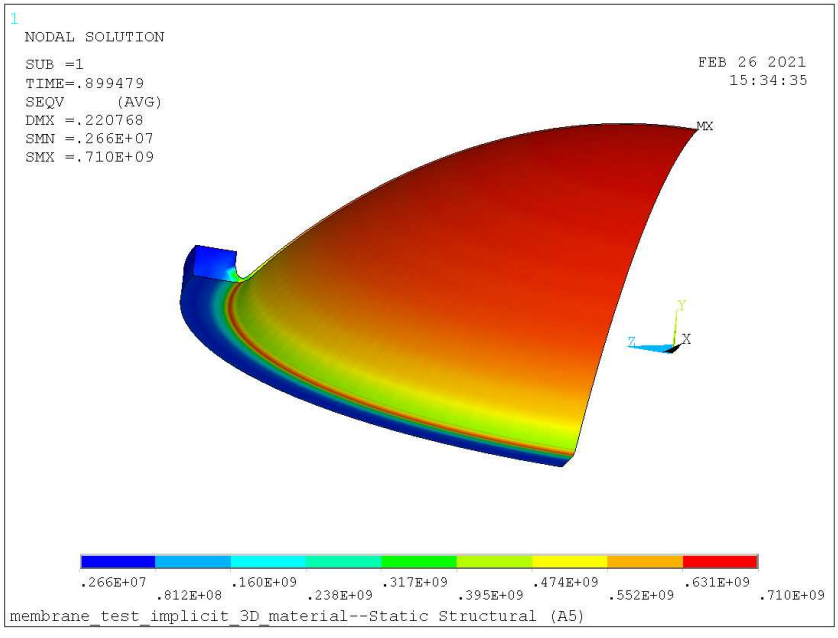

Figure 7. Equivalent Stress at 89.94% of the load.

In Figure 7, we can see the maximum stress at the center of the membrane (top in the figure). The thickness reductions are also stress concentration zones, but the center of the membrane has higher stresses.

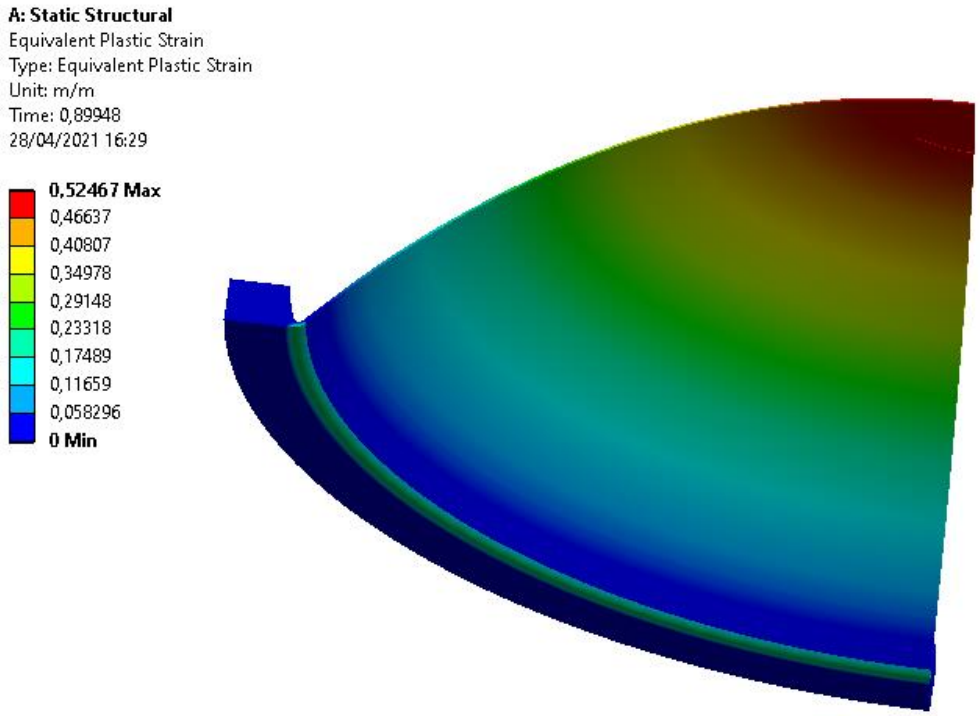

Figure 8. Equivalent Plastic Strains at 89.94 % of the load.

In Figure 8, unscaled deformation, we can see up to 52.4% plastic strain (EPS).

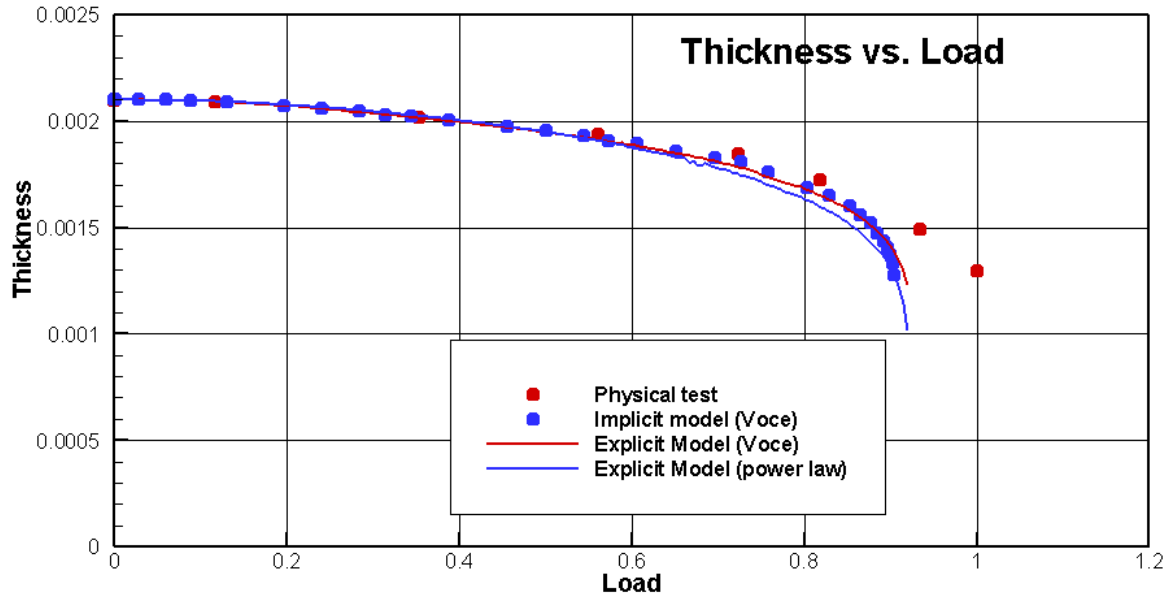

Figure 9. Comparison of load vs. thickness at the center, physical test vs. modelling.

In Figure 9, before the load reaches 89.94%, we can see a change in the thickness reductions, which becomes more drastic and unstable, until the point at which the model does not converge. These results are in accordance with the phenomenon of plastic instability.

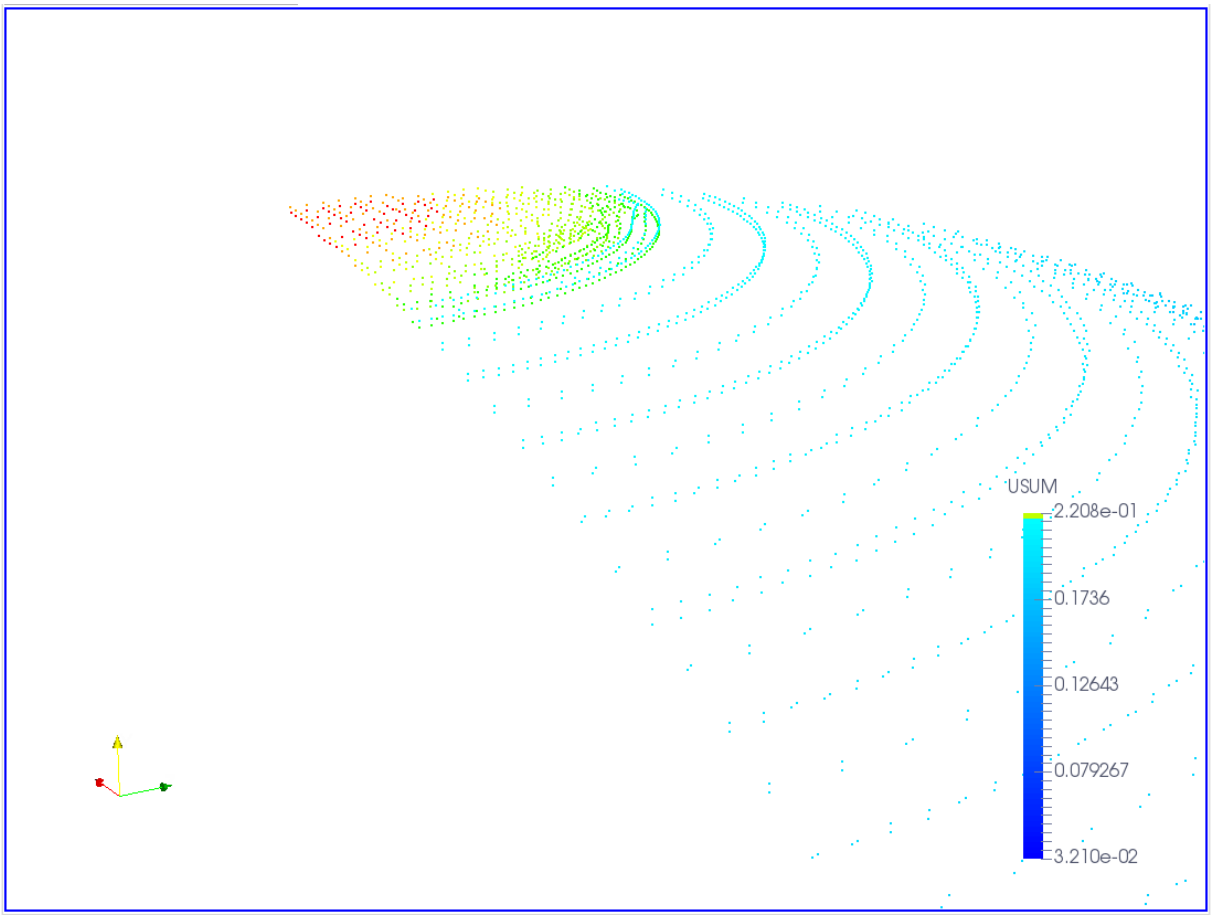

Figure 10. Contour plot of Total Deformation at the nodes.

In Figure 10 the deformation results are plotted (in m) at the nodes level. In this figure, the plastic collapse (thickness reduction) zone is drawn in red. The upper surface nodes and the lower surface nodes have differences in deformation, which is amplified by the difference in colors (red to orange). Thus, the thickness reduction from approximately 20 to 13 mm is clearly seen in the red area.

6 QUASI-STATIC EXPLICIT ANALYSIS

The same case was run with the explicit Code Simpact (REF?). The elements on the shell part are solid-shell elements with reduced integration (Flores, 2016) with 1 integration point in-plane and 5 trough-the-thickness. In the border of the model, the elements are standard solids with 4 integration points

In the case of explicit analysis, the material Voce model was run, but also the unsaturated model (Ludvik-Nadai Power Law) was run, for comparison purposes.

It can be noticed that the results obtained with both isotropic hardening models are very similar, although it must be noticed that, since they are different curves, there is a range in

which the saturation hardening is higher, for this reason the effective plastic strains are lower, but at the same time, the derivative of the hardening curve is lower in the Voce model, due to this there is a larger area where the stress are almost constant in the central zone.

Figures 11 and 12 show the effective plastic strain and the von Mises stress over the upper surface for a maximum displacement u_{max} = 0.20 m for a load factor of λ = 0.9.)

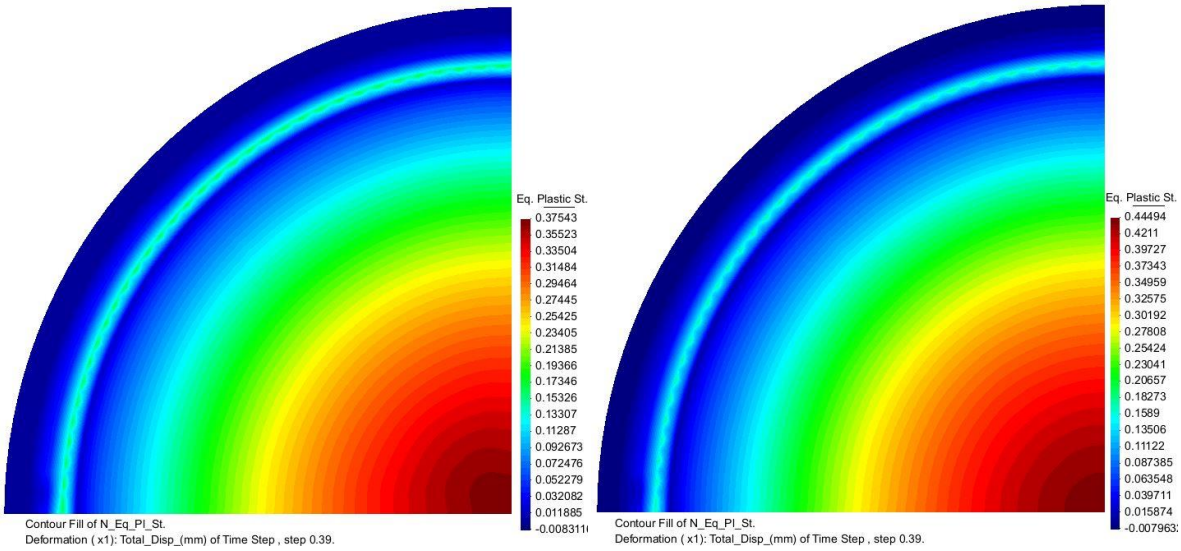

(a) (b)

Figure 11. Equivalent Plastic Strains at 90% of load. (a) Voce (b) Power Law

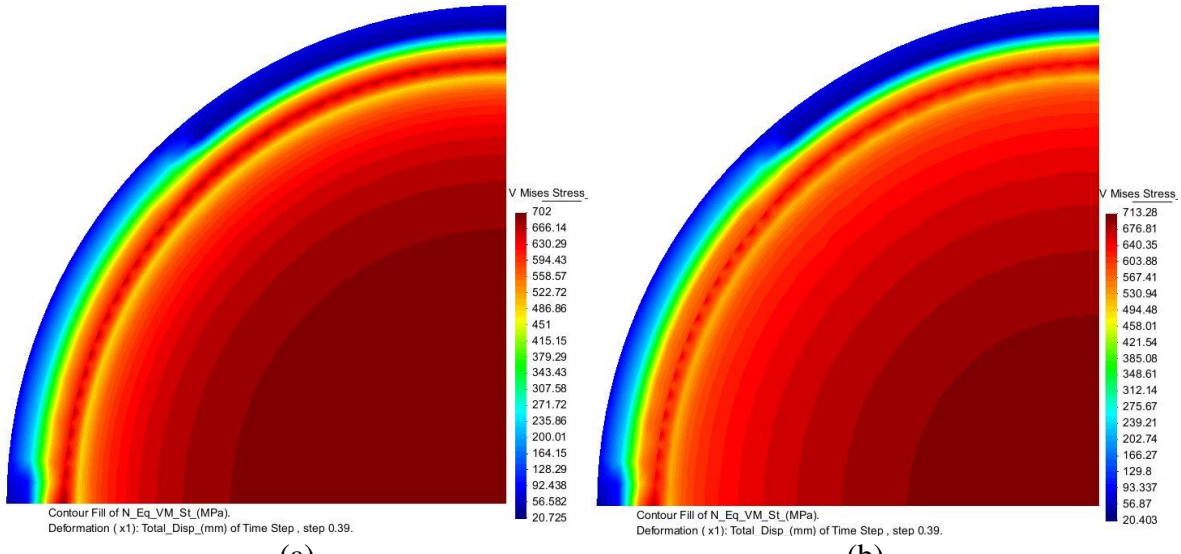

(a) (b)

Figure 12. von Mises Stress at 90% of load. (a) Voce (b) Power Law

Figure 9 above shows the thickness at the apex as the load increases, comparison with the implicit approach indicates minor differences. A retard due to dynamic effects was expected, but no retard was significantly noticeable.

7 CONCLUSIONS

The modelling of the static test has been performed with both 3D and solid-shell elements, and the results found are comparable with the 1987 physical tests.

As confirmed in the referenced work in 1987, the collapse loads are significantly higher than the values obtained by applying ASME appendices, since the latter are based on a uniaxial stress test.

This work points out that current-technology elements are capable of modelling very large plastic strains with material constitutive models that lead to plastic collapse of membranes, and the thickness reduction clearly signals the collapse areas, without the need of crack propagation models.

The results obtained by FEM could be compared to Forming Limit Diagrams, and this way obtain a much more quantifiable result relative to collapse.

REFERENCES

Berman, I. (1978). Inelasticity and the ASME Code. *Nuclear Engineering and Design*, *46*(2), 335–348. https://doi.org/10.1016/0029-5493(78)90019-5

Flores, F. G. (2016). A simple reduced integration hexahedral solid-shell element for large strains. *Computer Methods in Applied Mechanics and Engineering*, *303*, 260–287. https://doi.org/10.1016/j.cma.2016.01.013

Göller, B., Krieg, R., Messemer, G., & Wolf, E. (1987). On the failure of spherical steel containments under excessive internal pressure. *Nuclear Engineering and Design*. https://doi.org/10.1016/0029-5493(87)90043-4

Krieg, R., Eberle, F., Göller, B., Gulden, W., design, J. K.-… engineering and, & 1984, undefined. (n.d.). Spherical steel containments of pressurized water reactors under accident conditions: Investigation program and first results. *Elsevier*. Retrieved April 7, 2021, from https://www.sciencedirect.com/science/article/pii/0029549384902681

Sanchez Sarmiento, G. S., Idelsohn, S. R., Cardona, A., & Sonzogni, V. (1985). Failure internal pressure of spherical steel containments. *Nuclear Engineering and Design*, *90*(2), 209–222. https://doi.org/10.1016/0029-5493(85)90010-X

The ASME, N. Y. (1969). *Criteria of the ASME Boiler and Pressure Vessel Code for Design by Analysis ... - American Society of Mechanical Engineers. Special Committee to Review the Code Stress Basis - Google Libros*. https://books.google.com.ar/books?id=bLNKmQEACAAJ&dq=criteria+for+the+asme+boiler+and+pressure+vessel+code+for+design+by+analysis+in+sections+III+and+VIII&hl=es&sa=X&ved=2ahUKEwjx_pKF5ezvAhVQH7kGHTngAaoQ6AEwAHoECAQQAQ

Flores, F.G. (2016) “Simpact, An Explicit Finite Element Program”, Version 7.2, Deparment of Structures, National University of Córdoba, Argentina.